

Analytical Methods

Accepted Manuscript



This is an *Accepted Manuscript*, which has been through the Royal Society of Chemistry peer review process and has been accepted for publication.

Accepted Manuscripts are published online shortly after acceptance, before technical editing, formatting and proof reading. Using this free service, authors can make their results available to the community, in citable form, before we publish the edited article. We will replace this *Accepted Manuscript* with the edited and formatted *Advance Article* as soon as it is available.

You can find more information about *Accepted Manuscripts* in the [Information for Authors](#).

Please note that technical editing may introduce minor changes to the text and/or graphics, which may alter content. The journal's standard [Terms & Conditions](#) and the [Ethical guidelines](#) still apply. In no event shall the Royal Society of Chemistry be held responsible for any errors or omissions in this *Accepted Manuscript* or any consequences arising from the use of any information it contains.

PAPER

A new rhodamine-based chemosensor for turn-on fluorescent detection of Fe³⁺

Cite this: DOI: 10.1039/x0xx00000x

Xiang Han, Dong-En Wang, Sheng Chen, Longlong Zhang, Yadan Guo and Jinyi Wang*

Received 00th January 2012,
Accepted 00th January 2012

DOI: 10.1039/x0xx00000x

www.rsc.org/

A new fluorescent probe RH-Fe based on rhodamine B lactam was developed as a colorimetric and fluorescent chemosensor for Fe³⁺. The optical feature of RH-Fe for Fe³⁺ was investigated by UV-vis absorption and fluorescence emission spectroscopy. Upon the addition of Fe³⁺, the RH-Fe displayed a distinct color change from colorless to pink and a significant fluorescence enhancement, which can be directly detected by the naked eye. The stoichiometry of RH-Fe to Fe³⁺ complex was found to be 1:1 and the detection limit was determined as low as 0.27 μM. The results suggest that the probe RH-Fe may provide a conveniently method for visual detection of Fe³⁺ with high sensitivity.

1. Introduction

In recent decades, considerable attention has been devoted for the heavy and transition metal ions because of their importance to the environment and biology.^{1,2} Iron is an essential element in living organisms and plays a cofactor role in many enzymatic reactions. Meanwhile, iron can also provide the oxygen-carrying capacity in hemoglobin.³ However, both its deficiency

and overload of relatively normal limits can induce serious disorders such as Alzheimer, Huntington, and Parkinson diseases.^{4,5} Therefore, seeking an effective method for iron detection is important.⁶⁻¹⁰

At present, there are many methods which were employed to detect metal ions, such as atomic absorption spectroscopy, spectrophotometry and voltammetry. However, these methods

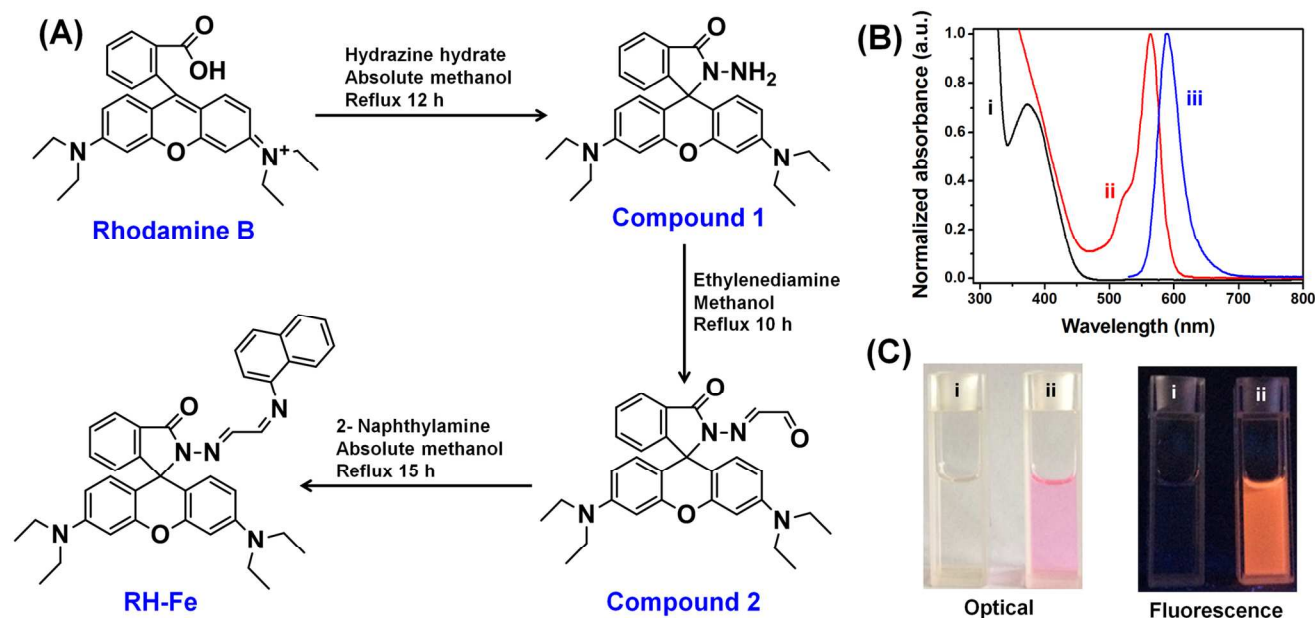


Figure 1. (A) The synthesis route and conditions for compound RH-Fe. (B) Normalized absorbance spectra of RH-Fe in the absence (i) and presence (ii) of Fe³⁺ and emission spectrum (iii) of RH-Fe in the presence of Fe³⁺. (C) The color and fluorescence changes before (i) and after (ii) the addition of Fe³⁺.

need expensive instruments and complex operation steps.¹¹⁻¹³ Compared with these methods, fluorescence-based methods are vital tools in metal ion detection and have been quickly developed due to the advantages of simple and easy operation, capability of visualization, high sensitivity and selectivity.¹⁴⁻¹⁹ Up to now, a great quantity of fluorescence-based sensors have been developed for the detection of various heavy metals or transition metals.²⁰⁻²⁴ However, only a few fluorescent probes for Fe³⁺ were reported. Bai and co-workers²⁵ reported four coumarin-based fluorescent sensors for Fe³⁺ detection. All of the four sensors displayed a selective fluorescence quenching effect to Fe³⁺. Among them, sensor 4 showed the most excellent selectivity for Fe³⁺ over a wide range of tested metal ions in acetonitrile. Liu and co-workers²⁶ reported a fluorescent probe L for Fe³⁺ with high sensitivity and selectivity over other heavy and transition metal ions in acetonitrile–water (98:2, v/v). The detection limit was as low as 60.4 nM. Jiang and co-workers²⁷ reported two fluorescent chemosensors based on anthracene and dansyl groups as fluorophores for Fe³⁺. Both of them displayed high selectivity and sensitivity towards Fe³⁺ over other metal ions in aqueous solution. Generally, the detection mechanism of the currently reported Fe³⁺ probes was based on the paramagnetic property of Fe³⁺, which could lead to fluorescence quenching, also, is not as sensitive as fluorescence enhancement.²⁸ Therefore, the development of novel fluorescent “turn-on” chemosensors for sensitive Fe³⁺ detection is still highly desired.²⁹

Rhodamine-based fluorophores have been widely developed and utilized for chemosensor applications because of their high extinction coefficient, excellent quantum yield, great photostability, and relatively long emission wavelength.³⁰ Under external stimulus, such as heavy metal ions or pH, rhodamine dyes change the closed loop lactam state into open-loop amide, accompanied by the generation of color change and fluorescence enhancement.³¹ In recent years, the utilization of rhodamine-based fluorescent dyes as a new type of “turn-on” fluorescence probes for metal ion detection is one of the hot research topics.³²⁻³⁶ Herein, a new rhodamine B-derived Fe³⁺ probe RH-Fe (Figure 1A) was designed and synthesized through the double schiff's base condensation between rhodamine B and 2-naphthylamine. The structure of RH-Fe was carefully characterized by ¹H-nuclear magnetic resonance (NMR), ¹³C-NMR and ESI-MS spectral measurements. RH-Fe was found to act as a reversible “turn-on” fluorescence chemosensor for Fe³⁺ detection with high sensitivity and selectivity in H₂O–CH₃CN (7:3 v/v) solution.

2. Experimental

2.1. Materials and apparatus

Rhodamine B was purchased from Alfa Aesar (Lancaster, England). 2-Naphthylamine and hydrazine hydrate were purchased from Aladdin (Shanghai, China). Dry solvents used in the synthesis were purified by using standard procedures. All other reagents and solvents were of analytical grade and

supplied by local commercial suppliers. Ultrapurified water was supplied by a Milli-Q system (Millipore). Reactions were monitored by thin-layer chromatography (TLC) using silica gel 60 GF254 (Qingdao Haiyang Chem. Co., Ltd., Shangdong, China). Column chromatography was conducted by using silica gel 60 (200–300 mesh) (Qingdao Haiyang Chem. Co., Ltd.).

¹H-nuclear magnetic resonance (NMR) and ¹³C-NMR spectra were recorded by using a BrukerAvance DMX 500 MHz/125 MHz spectrometer (Bruker, Billerica, MA, USA). Peaks were based on a tetramethylsilane (TMS) internal standard. Electrospray ionization mass spectroscopy (ESI-MS) data were obtained by using a Thermo Scientific LCQ FLEET mass spectrometer equipped with an electrospray ion source and controlled by Xcalibur software (Thermo Fisher Scientific, Waltham, MA, USA). UV-vis absorption spectra were recorded on a Shimadzu UV1800 spectrometer (Shimadzu, Kyoto, Japan). Fluorescence emission spectra were obtained on a Shimadzu RF-5301PC fluorescence spectrometer (Shimadzu).

2.2. Synthesis of compound 1

Rhodamine B (248.5 mg, 0.51 mmol), hydrazine hydrate (1 mL) and anhydrous methanol (15 mL) were placed in a round flask. The resulting mixture was refluxed and stirred for 12 h. After cooling to room temperature, the reaction mixture was poured into HCl (1 N) to dissolve the solids. Then, NaOH (1 N) was added to the mixture and a red solid precipitation formed. The precipitate was filtered, washed with water and dried in vacuo to obtain compound 1 as a brick red solid (204.5 mg) in 80.1% yield. ¹H NMR (500 MHz, CDCl₃) δ (ppm): 7.84-7.85 (t, 1H), 7.36-7.38 (t, 2H), 7.02-7.04 (t, 1H), 6.35-6.40 (m, 4H), 6.21-6.23 (q, 2H), 3.62 (s, 2H), 3.24-3.29 (q, 8H), 1.08-1.11 (t, 12H). ¹³C NMR (125 MHz, CDCl₃) δ (ppm): 166.15, 153.90, 151.60, 148.94, 132.50, 130.10, 128.11, 123.86, 123.01, 108.09, 104.70, 98.05, 65.92, 44.40, 12.64.

2.3. Synthesis of compound 2

To a solution of ethylenediamine (3 mL) in anhydrous methanol (15 mL) was added compound 1 (1.20 g, 2.62 mmol). The resulting mixture was refluxed and stirred for 10 h to produce a clear yellow solution. The solvent was removed under reduced pressure. The crude product was purified by column chromatography on silica gel (ethyl acetate: petroleum ether: triethylamine = 100:10:1, v/v/v) to afford compound 2 as a yellow solid in 90.8% yield. ¹H NMR (500 MHz, CDCl₃) δ (ppm): 9.45-9.46 (d, 1H), 8.03-8.05 (d, 1H), 7.48-7.44 (m, 3H), 7.10-7.19 (d, 1H), 6.40-6.46 (m, 4H), 6.24-6.26 (q, 2H) 3.31-3.35 (q, 8H), 1.15-1.18 (t, 12H). ¹³C NMR (125 MHz, CDCl₃) δ (ppm): 192.70, 165.99, 152.65, 149.31, 141.25, 135.00, 128.65, 127.55, 126.61, 124.10, 108.24, 103.81, 98.15, 66.70, 44.38, 12.61.

2.4. Synthesis of RH-Fe

2-Naphthylamine (65 mg, 0.45 mmol), compound 2 (225 mg, 0.45 mmol) and absolute ethanol (10 mL) were placed in a round flask under nitrogen gas. The reaction mixture was refluxed and stirred for 15 h to afford a yellow precipitate. The

precipitate was filtered and washed with small amount of ice ethanol. The crude product was purified by column chromatography on silica gel (ethyl acetate: petroleum ether = 10:1, v/v) to obtain RH-Fe as a yellow solid in 32.4% yield. ^1H NMR (500 MHz, CDCl_3) δ (ppm): 8.29-8.31 (d, 1H), 8.25-8.26 (d, 1H), 8.19-8.21 (d, 1H), 8.07-8.09 (d, 1H), 7.83-7.85 (d, 1H), 7.71-7.73 (d, 1H), 7.53-7.57 (t, 1H), 7.48-7.52 (m, 3H), 7.41-7.44 (t, 1H), 7.16-7.18 (d, 1H), 6.99-7.00 (d, 1H), 6.60-6.61 (d, 2H), 6.52-6.53 (d, 2H), 6.33-6.36 (dd, 2H), 3.37-3.42 (q, 8H), 1.21-1.24 (t, 12H). ^{13}C NMR (125 MHz, CDCl_3) δ (ppm): 165.84, 160.44, 152.88, 149.12, 148.26, 145.61, 134.25, 127.66, 127.62, 126.63, 126.37, 125.95, 125.80, 123.89, 123.13, 112.87, 108.25, 105.05, 98.39, 66.11, 44.39, 12.65. ESI-MS m/z : calculated 621.77, found $[\text{M}+\text{H}^+]$, 622.61.

2.5. UV-Vis absorption and fluorescence measurements

Stock solutions (0.1 M) of metal ions in water were prepared from KCl, NaCl, $\text{MgCl}_2 \cdot 6\text{H}_2\text{O}$, PbCl_2 , $\text{CuSO}_4 \cdot 5\text{H}_2\text{O}$, $\text{Zn}(\text{NO}_3)_2 \cdot 6\text{H}_2\text{O}$, $\text{CaCl}_2 \cdot 2\text{H}_2\text{O}$, $\text{Ni}(\text{NO}_3)_2 \cdot \text{H}_2\text{O}$, HgCl_2 , $\text{MnSO}_4 \cdot \text{H}_2\text{O}$, $\text{Cd}(\text{NO}_3)_2 \cdot 4\text{H}_2\text{O}$, $\text{CoCl}_2 \cdot 6\text{H}_2\text{O}$, $\text{FeCl}_2 \cdot 4\text{H}_2\text{O}$, $\text{Al}(\text{NO}_3)_3 \cdot 9\text{H}_2\text{O}$, $\text{Fe}(\text{NO}_3)_3 \cdot 9\text{H}_2\text{O}$, $\text{CrCl}_3 \cdot 6\text{H}_2\text{O}$, $\text{BaCl}_2 \cdot 2\text{H}_2\text{O}$ and AgNO_3 . Stock solutions (0.1 M) of anions in water were prepared from NaCl, NaF, NaBr, NaNO_3 , NaNO_2 , NaN_3 , Na_2SO_4 , Na_2SO_3 , Na_2HSO_3 , $\text{Na}_2\text{S}_2\text{O}_3 \cdot 5\text{H}_2\text{O}$, CH_3COONa , Na_2CO_3 and NaHCO_3 . RH-Fe was exactly weighted and dissolved in acetonitrile to afford the probe stock solution (1 mM). For colorimetric and fluorescent detection of Fe^{3+} , the stock solution of RH-Fe was diluted with $\text{H}_2\text{O}-\text{CH}_3\text{CN}$ (7:3, v/v) to obtain a 10 μM or 20 μM working solution. Then, different concentrations of Fe^{3+} were mixed with 3 mL of the working solution in a 1 cm cuvette. Unless otherwise stated, all the spectral studies were performed in $\text{H}_2\text{O}-\text{CH}_3\text{CN}$ (7:3, v/v) solution at room temperature. The fluorescence excitation wavelength was at 520 nm, with an emission wavelength range from 530 nm to 800 nm. Both the excitation and emission slit widths were 3 nm.

3. Results and discussion

3.1. Synthesis of the probe RH-Fe

The probe RH-Fe was synthesized by a three-step reaction with a total yield of 23.6% according to the route shown in Figure 1A. Compound 1 was readily obtained by the reaction of rhodamine B with hydrazine hydrate in methanol with a satisfied yield of 80.1%. Then, 2-naphthylamine was directly linked to compound 2 through the typical Schiff's base condensation reaction to afford the probe RH-Fe in the yield of 32.4%. The chemical structure of RH-Fe was carefully characterized by ^1H NMR, ^{13}C NMR and ESI-MS. The detailed synthetic procedures and relevant spectral data are given in the experimental section and supplementary information (Figures S4-S10, in the ESI†).

3.2. The selectivity and sensitivity of RH-Fe for Fe^{3+} detection

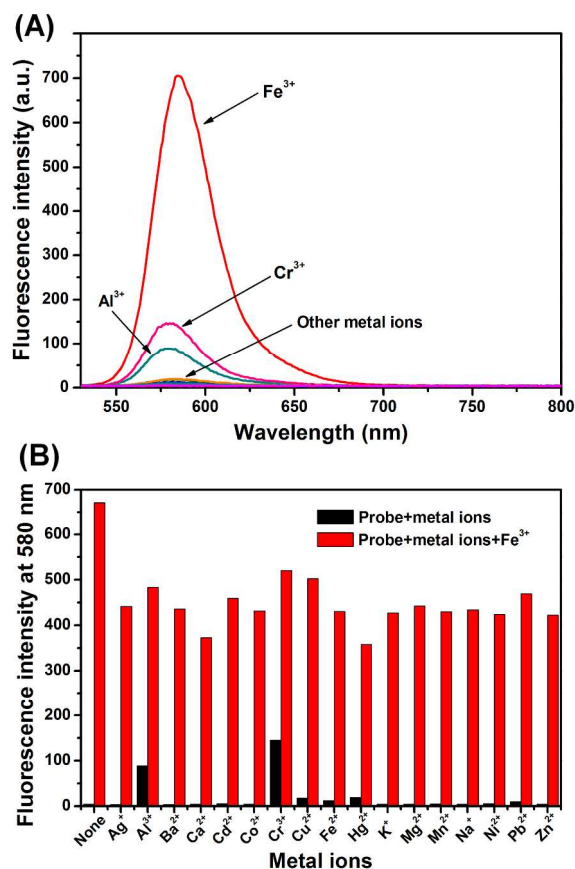


Figure 2. (A) Fluorescence spectra of RH-Fe (20 μM) in the presence of different metal ions (200 μM). (B) Fluorescence responses of RH-Fe (20 μM) upon the addition of various metal ions (200 μM) (black column), and upon subsequent addition of Fe^{3+} (red column).

Fluorescence and UV absorption studies were first performed. As shown in Figure 1B, normalized absorption spectra of RH-Fe, RH-Fe with Fe^{3+} , and emission spectrum of RH-Fe with Fe^{3+} were collected. The probe RH-Fe shows a maximum absorbance at 376 nm in the absence of Fe^{3+} (the black line), suggesting that the closed spirolactone form of Rhodamine B presented.³⁷ Upon the addition of Fe^{3+} , a new absorption band at 561 nm appeared in the visible range (the blue line), accompanied by a color change from colorless to pink (Figure 1C, left). Excitation of the RH-Fe solution with Fe^{3+} produced a strong fluorescence emission at 580 nm (the red line in Figure 1B, and Figure 1C, right). The results clearly indicate that the rhodamine B ring-open amide form was produced in the presence of Fe^{3+} . The fluorescence quantum yield was measured to be 0.24 (Table S1†) with rhodamine B in ethyl alcohol as the standard, consistent with the literature value.³⁸

To research the selectivity of RH-Fe, various metal ions including Na^+ , Zn^{2+} , Mn^{2+} , Pd^{2+} , K^+ , Ni^{2+} , Mg^{2+} , Ba^{2+} , Cd^{2+} , Ca^{2+} , Ag^+ , Co^{2+} , Hg^{2+} , Cu^{2+} , Fe^{2+} , Fe^{3+} , Al^{3+} and Cr^{3+} were chosen to add into the probe solutions. As shown in the supplementary Figure S1, only the addition of Fe^{3+} immediately induced a clear color change from colorless to pink, while the addition of other metal ions such as Na^+ , Zn^{2+} , Mn^{2+} , Pd^{2+} , K^+ ,

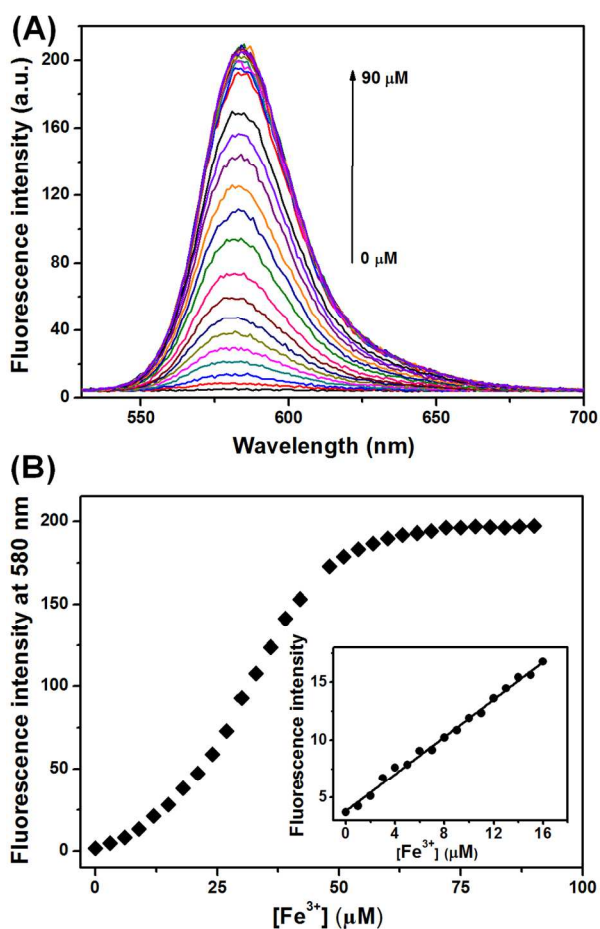


Figure 3. (A) Fluorescence spectra of RH-Fe (20 μM) upon the addition of increasing amount of Fe^{3+} (0-90 μM). Both the excitation and emission slit were 3 nm. (B) Fluorescence intensity changes at 580 nm of RH-Fe (20 μM) as a function of Fe^{3+} concentration. Inset: the linear relationship of RH-Fe between the fluorescence intensity and Fe^{3+} concentration.

Ni^{2+} , Mg^{2+} , Ba^{2+} , Cd^{2+} , Ca^{2+} , Ag^+ , Co^{2+} , Hg^{2+} , Cu^{2+} , Fe^{2+} , Al^{3+} and Cr^{3+} did not show any color changes, revealing the potential application of RH-Fe as a naked-eye chemosensor for the detection of Fe^{3+} in real-time. The selectivity properties of RH-Fe were further monitored by UV-visible absorption and fluorescence emission spectra. As shown in Figure 2A and Figure S2 in the ESI†, the addition of Fe^{3+} can produce a large 170-fold increase in fluorescence emission intensity and a dramatic 260-fold increase in absorption band. However, the other metal ions, such as Na^+ , Zn^{2+} , Mn^{2+} , Pd^{2+} , K^+ , Ni^{2+} , Mg^{2+} , Ba^{2+} , Cd^{2+} , Ca^{2+} , Ag^+ , Co^{2+} , Hg^{2+} , Cu^{2+} and Fe^{2+} , did exhibit negligible variation in absorption and emission spectra. It should be noted that the addition of Al^{3+} and Cr^{3+} could cause small changes in absorption and emission spectra. However, the effects are quite mild compared with Fe^{3+} , because Fe^{3+} could lead to great enhancement in absorption and fluorescence emission which were about 4 times than that of Al^{3+} and Cr^{3+} . In general, the characteristics of Fe^{3+} , Al^{3+} and Cr^{3+} are quite similar and it can be found that Al^{3+} and Cr^{3+} are able to affect the Fe^{3+} selective chemosensors in many previous reported rhodamine-based spirolactam probes.³⁹

A competition experiment was further carried out by adding Fe^{3+} to RH-Fe solution containing other metal ions, and the results are shown in Figure 2B. Before the introduction of Fe^{3+} , there were almost no fluorescence signals at 580 nm in the presence of other metal ions, except Al^{3+} and Cr^{3+} (the addition of the two ions induced relative weak fluorescence intensities). When 10 eq. of Fe^{3+} were introduced to the above solutions, remarkable enhancement in fluorescence emission intensities at 580 nm was observed. These interesting features clearly demonstrated that RH-Fe can be served as a selective “naked-eye” chemosensor for Fe^{3+} .

The fluorescence spectra of RH-Fe upon titration with Fe^{3+} were then performed (Figure 3A). The fluorescence intensity of RH-Fe (10 μM) at 580 nm was gradually increased with the addition of increasing amount of Fe^{3+} (0 μM – 90 μM). The enhanced intensity of RH-Fe displayed a good linear regression relationship ($R^2 = 0.994$) with the concentration of Fe^{3+} in the range of 1 to 16 μM based on the titration experiment (Figure 3B, inset). The limit of detection (LOD) of RH-Fe for Fe^{3+} was estimated to be as low as 0.27 μM based on $3\sigma/S$ (see the ESI†). Admittedly, this LOD is below the upper limit of Fe^{3+} level in drinking water set by World Health Organization, which is ca. 5 μM .⁴⁰ Compared with the previous studies (Table

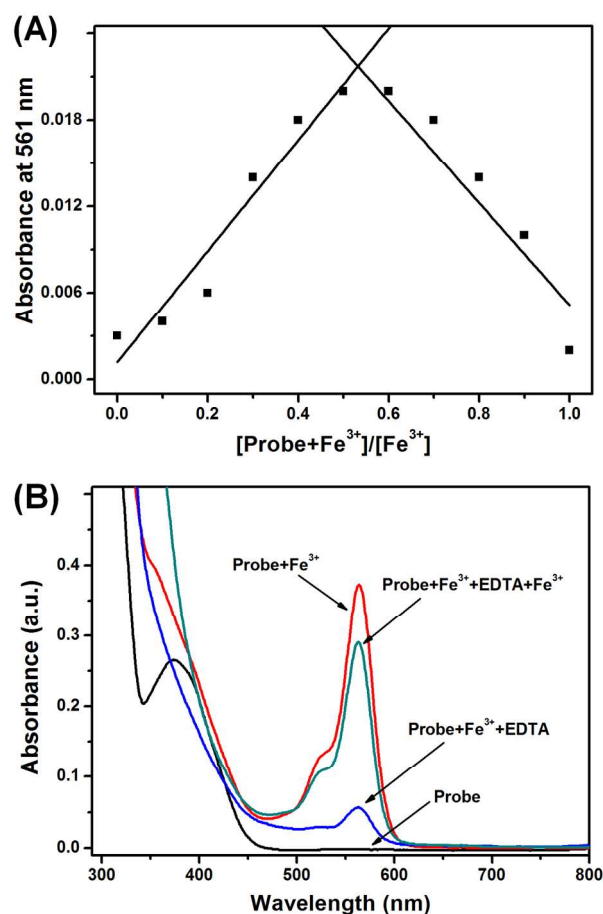


Figure 4. (A) Job's plots according to the continuous variations method. The total concentration of RH-Fe and Fe^{3+} is 20 μM . (B) Reversible absorbance spectral response of RH-Fe to Fe^{3+} .

S3[†]), the probe RH-Fe had the lower detection limit. The results imply that the probe RH-Fe can be used as a sensitive chemosensor for the detection of Fe³⁺ in micromolar range.

3.3. The mechanism of RH-Fe for Fe³⁺ detection

To understand the binding stoichiometry between RH-Fe and Fe³⁺, the Job's plot experiment was carried out (Figure 4A) using the continuous variation method.^{41,42} The result demonstrated that RH-Fe could form a 1:1 complex with Fe³⁺ and the binding constant K_a of RH-Fe with Fe³⁺ was calculated to be $0.25 \times 10^4 \text{ M}^{-1}$ according to the Benesi-Hildebrand equation (Figure S3, in the ESI[†]), suggesting that the probe RH-Fe is able to well binding Fe³⁺ with a good binding affinity. ESI-MS analysis showed that [RH-Fe + H⁺] has a molecular ion peak at $m/z = 622.61$. Upon the addition of Fe³⁺, a peak at $m/z = 773.49$ [RH-Fe + Fe³⁺ + 4H₂O + Na⁺] appeared (Figure S11, in the ESI[†]). The observation indicated that RH-Fe bound with Fe³⁺ in a 1:1 binding. More importantly, the formation of RH-Fe-Fe³⁺ complex is promptly completed in seconds and the binding process is reversible. The reversible binding mode of RH-Fe with Fe³⁺ was verified with the EDTA titration

method.⁴³ EDTA is well known metal ligand compound and could strongly bind with Fe³⁺. Upon addition of 10 eq. of EDTA to the solution of 20 μM RH-Fe with Fe³⁺ (10 eq.), the absorption intensity at 561 nm was almost completely quenched (Figure 4B) due to the much strong complex binding between EDTA and Fe³⁺ ions, which would destroy the RH-Fe-Fe³⁺ complex. Further addition of 15 eq. of Fe³⁺ to the solution gave a 78.2% recovery in the absorbance intensity (the green line), indicating the excessive Fe³⁺ formed RH-Fe-Fe³⁺ complex with the probe RH-Fe again. The results indicate that the probe RH-Fe has the ability to reversibly detect Fe³⁺. Based on the above results, a schematic figure of the proposed binding mechanism of the probe RH-Fe for Fe³⁺ is described in the supplementary Scheme S1. The carbonyl oxygen, imino nitrogen and 2-naphthylamine nitrogen are anticipated to act as metal ligands for Fe³⁺ binding.⁴⁴⁻⁴⁶ The strong binding interactions between RH-Fe and Fe³⁺ thus caused the chelation-induced ring opening of rhodamine spirolactam, which produced the discoloration and fluorescence enhancement.

3.4. The effect of pH and anions on RH-Fe for Fe³⁺ detection

The stability of the probe RH-Fe in acidic or basic condition is very important for practical applications. In the current study, the pH effect on RH-Fe sensing property was investigated (Figure 5A) to find a suitable pH range under which RH-Fe could selectively and efficiently detect Fe³⁺. The probe RH-Fe solutions don't show the characteristic absorption of rhodamine at 561 nm between pH 5.54 and 13.55 in the absence of Fe³⁺, which suggests that the spirolactam tautomer of RH-Fe is insensitive to pH change over this range. When pH < 5.54, gradual increase of the absorption at 561 nm was observed, which could be ascribed to the acid-induced ring opening of rhodamine spirolactam.³² However, the addition of Fe³⁺ led to strong absorption enhancement at a comparatively wide pH range (5.54–10.12). The result clearly indicates that the probe RH-Fe can be used in a broad range of pH (5.54–10.12).

The effect of other anions on the sensing property of RH-Fe for Fe³⁺ was also investigated (Figure 5B). No interferences were observed with Br⁻, Cl⁻, CO₃²⁻, F⁻, HCO₃²⁻, HSO₃²⁻, S₂O₃²⁻, NO₃⁻ and SO₃²⁻ after adding Fe³⁺ in the probe solutions. AcO⁻ and SO₄²⁻ showed minor interferences to RH-Fe for Fe³⁺ detection. While N₃⁻ and NO₂⁻ gave the remarkable interferences relative to the other anionic. These results further demonstrate that RH-Fe can be served as a selective and sensitive chemosensor for Fe³⁺ under various conditions.

3.5. Analysis of Fe³⁺ in real samples using probe RH-Fe

In the terms of simplicity and sensitivity, the probe RH-Fe was then practically utilized to estimate the concentration of Fe³⁺ in real samples. The water samples collected from Weihe River and local tap water were spiked into the aliquot of Fe³⁺. The recovery experiments were then performed. As summarized in the supplementary Table S2[†], the recoveries of Fe³⁺ are range from 77.3 % to 113.6 % in tap water and 88.5 % to 112.8 % in Weihe River. The results show that RH-Fe has the potential application for quantitative detection of Fe³⁺ in real samples.

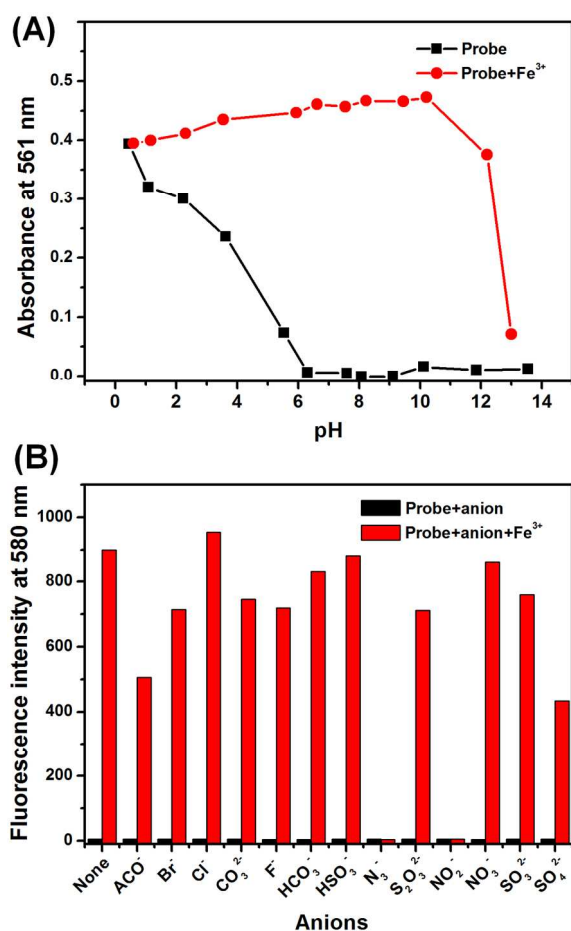


Figure 5. (A) Absorbance changes at 561 nm of RH-Fe (20 μM) as a function of pH. (B) Fluorescence intensity changes at 580 nm of RH-Fe (20 μM) upon addition of Fe³⁺ (100 μM) in the presence of different anions (200 μM).

4. Conclusion

In summary, we have synthesized a “double schiff’s base” probe RH-Fe as a new fluorescent turn-on chemosensor for Fe³⁺. The probe displayed distinct color change from colorless to pink and significant fluorescence enhancement upon the addition of Fe³⁺. Also, RH-Fe showed high selectivity and sensitivity for Fe³⁺ in the presence of various metal ions and anions. The complex stoichiometry of RH-Fe with Fe³⁺ was found to be 1:1 by the Job’s plot. The detection limit of RH-Fe for Fe³⁺ was calculated to be as low as 0.27 μM. In addition, the feasibility of RH-Fe for Fe³⁺ detection in real samples was exemplified. The results demonstrate that the probe RH-Fe can be served as a sensitive, selective and naked-eye chemosensor for Fe³⁺ detection.

Acknowledgements

This work was supported by the National Natural Science Foundation of China (21175107 and 21375106) and the Fundamental Research Funds for the Central Universities (Z109021303).

Notes and references

College of Science, Northwest A&F University, Yangling, Shaanxi 712100, P. R. China. Fax: +86-298-708-2520; Tel: +86-298-708-2520; Email: jywang@nwsuaf.edu.cn

†Electronic Supplementary Information (ESI) available: Materials and methods, supplementary Figs. S1–S11, Tables S1–S3 and Scheme S1. See DOI: 10.1039/b000000x/

References

1. A. Chatterjee, M. Santra, N. Won, S. Kim, J. K. Kim, S. B. Kim and K. H. Ahn, *J. Am. Chem. Soc.*, 2009, **131**, 2040.
2. L. Yuan, W. Lin and Y. Feng, *Org. Biomol. Chem.*, 2011, **9**, 1723.
3. M. Kumar, R. Kumar, V. Bhalla, P. R. Sharma, T. Kaur and Y. Qurishi, *Dalton Trans.*, 2012, **41**, 408.
4. M. Zheng, H. Tan, Z. Xie, L. Zhang, X. Jing and Z. Sun, *ACS Appl. Mater. Inter.*, 2013, **5**, 1078.
5. H. Kozłowski, A. Janicka-Kłos, J. Brasun, E. Gaggelli, D. Valensin and G. Valensin, *Coordin. Chem. Rev.*, 2009, **253**, 2665.
6. M. She, Z. Yang, B. Yin, J. Zhang, J. Gu, W. Yin and Z. Shi, *Dyes Pigments*, 2012, **92**, 1337.
7. G. Sivaraman, V. Sathiyaraja and D. Chellappa, *Luminescence*, 2014, **145**, 480.
8. X. F. Bao, J. X. Shi, X. M. Nie, B. J. Zhou, X. L. Wang, L. Y. Zhang, H. Liao and T. Pang, *Bioorg. Med. Chem. Lett.*, 2014, **22**, 4825.
9. T. M. Geng, R. Y. Huang and D. Y. Wu, *RSC Adv.*, 2014, **4**, 46332.
10. D. En, Y. Guo, B. T. Chen, B. Dong and M. J. Peng, *RSC Adv.*, 2014, **4**, 248.
11. A. Ohashi, H. Ito, C. Kanai, H. Imura and K. Ohashi, *Talanta*, 2005, **65**, 525.
12. S. Lunvongsa, M. Oshima and S. Motomizu, *Talanta*, 2006, **68**, 969.
13. A. Bobrowski, K. Nowak and J. Zarębski, *Anal. Bioanal. Chem.*, 2005, **382**, 1691.
14. B. Bag and A. Pal, *Org. Biomol. Chem.*, 2011, **9**, 4467.
15. M. J. Yuan, Y. L. Li, J. B. Li, C. H. Li, X. F. Liu, J. Lv, J. L. Xu, H. B. Liu, S. Wang and D. B. Zhu, *Org. Lett.*, 2007, **9**, 2313.
16. M. Zhu, M. J. Yuan, X. F. Liu, J. L. Xu, J. Lv, C. S. Huang, H. B. Liu, Y. L. Li, S. Wang and D. B. Zhu, *Org. Lett.*, 2008, **10**, 1481.
17. T. Anand, G. Sivaraman, A. Mahesh and D. Chellappa, *Anal. Chim. Acta*, 2015, **853**, 596.
18. T. Anand, G. Sivaraman and D. Chellappa, *J. Photoch. Photobio. A*, 2014, **281**, 47.
19. G. Sivaraman, T. Anand and D. Chellappa, *Anal. Methods*, 2014, **6**, 2343.
20. K. Bera, A. K. Das, M. Nag and S. Basak, *Anal. Chem.*, 2014, **86**, 2740.
21. L. Zhou, X. Zhang, Q. Wang, Y. Lv, G. Mao, A. Luo and W. Tan, *J. Am. Chem. Soc.*, 2014, **136**, 9838.
22. S. Sun, B. Qiao, N. Jiang, J. Wang, S. Zhang and X. Peng, *Org. Lett.*, 2014, **16**, 1132.
23. E. Karakuş, M. Üçüncü and M. Emrulloğlu, *Chem. Commun.*, 2014, **50**, 1119.
24. G. F. Chen, H. M. Jia, L. Y. Zhang, J. Hu, B. H. Chen, Y. L. Song and G. Y. Bai, *Res. Chem. Intermediate.*, 2013, **39**, 4081.
25. L. W. Zhang and X. Liu, *New J. Chem.*, 2013, **37**, 821.
26. L. Fu, J. Mei, J. T. Zhang, Y. Liu and F. L. Jiang, *Luminescence*, 2013, **28**, 602.
27. J. L. Bricks, A. Kovalchuk, C. Trieflinger, M. Nofz, M. Bueschel and L. Tolmachev, *J. Am. Chem. Soc.*, 2005, **127**, 13522.
28. M. Zheng, H. Tan, Z. Xie, L. Zhang, X. Jing and Z. Sun, *ACS Appl. Mater. Inter.*, 2013, **5**, 1078.
29. S. Pal, N. Chatterjee and P. K. Bharadwaj, *RSC Adv.*, 2014, **4**, 26585.
30. H. N. Kim, M. H. Lee, H. J. Kim, J. S. Kim and J. Yoon, *Chem. Soc. Rev.*, 2008, **37**, 1465.
31. X. Q. Zhan, Z. H. Qian, H. Zheng, B. Y. Su, Z. Lan and J. G. Xu, *Chem. Commun.*, 2008, **16**, 1859.
32. W. D. Chen, W. T. Gong, Z. Q. Ye, Y. Lin and G. L. Ning, *Dalton Trans.*, 2013, **42**, 10093.
33. G. Sivaraman, T. Anand and D. Chellappa, *Analyst*, 2012, **137**, 5881.
34. G. Sivaraman and D. Chellappa, *J. Mater. Chem. B*, 2013, **1**, 5768.
35. G. Sivaraman, B. Vidya and D. Chellappa, *RSC Adv.*, 2014, **4**, 30828.
36. G. Sivaraman, T. Anand and D. Chellappa, *ChemPlusChem*, 2014, **79**, 1761.
37. M. I. Rodríguez-Cáceres, R. A. Agbaria and I. M. Warner, *J. Fluoresc.*, 2005, **15**, 185.
38. X. Zheng, W. Zhang, L. Mu, X. Zeng, S. Xue, Z. Tao and T. Yamatob, *J. Incl. Phenom. Macro.*, 2010, **68**, 139.
39. R. Kagit, M. Yildirim, O. Ozay, S. Yesilot and H. Ozay, *Inorg. Chem.*, 2014, **53**, 2144.
40. C. Y. Huang, *Meth. Enzymol.*, 1982, **87**, 509.
41. M. S. Yuan, Q. Wang, W. Wang, D. E. Wang, J. R. Wang and J. Wang, *Analyst*, 2014, **139**, 1541.
42. J. H. Ye, J. Liu, Z. Wang, Y. Bai, W. Zhang and W. He, *Tetrahedron Lett.*, 2014, **55**, 3688.
43. L. Yuan, W. Lin and Y. Feng, *Org. Biomol. Chem.*, 2011, **9**, 1723.
44. S. Z. Ji, X. M. Meng, W. P. Ye, Y. Feng, H. T. Sheng, Y. L. Cai, J. S. Liu, X. F. Zhu and Q. X. Guo, *Dalton Trans.*, 2014, **43**, 1583.
45. N. R. Chereddy, K. Saranraj, A. K. Barui, C. R. Patra, V. J. Rao and S. Thennarasu, *RSC Advances*, 2014, **4**, 24324.

- 1
2
3
4
5
6
7
8
9
10
11
12
13
14
15
16
17
18
19
20
21
22
23
24
25
26
27
28
29
30
31
32
33
34
35
36
37
38
39
40
41
42
43
44
45
46
47
48
49
50
51
52
53
54
55
56
57
58
59
60
46. N. R. Chereddya, K. Sumana, P. S. Korrapatib, S. Thennarasu and A. B. Mandal, *Dyes Pigments*, 2012, **95**, 606.